ELSEVIER

Journal of Alloys and Compounds 253–254 (1997) 452–458

Journal of ALLOYS AND COMPOUNDS

Surface properties of the fluorinated La-incorporated Ti/Zr-based AB_2 laves phase alloys

F.-J. Liu*, H. Ota, S. Okamoto, S. Suda

Department of Chemical Engineering, Kogakuin University, 2665-1, Nakano-machi, Hachioji-shi, Tokyo 192, Japan

Abstract

A new class of fluorinated Ti/Zr-based AB_2 laves phase alloys with an extremely high reactivity to hydrogen was demonstrated by incorporating a small amount of rare earth metals such as La. Great benefits on improving the activation characteristics both in gas–solid and liquid–solid reactions were demonstrated. This is known to contribute to the formation of the La-fluoride layer on those La-enriched secondary phases homogeneously distributed at the grain boundaries of the AB_2 matrix. This research is based on a fluorination procedure invented in our laboratory in 1991 by using an aqueous F^--ion containing solution (F-solution) to form a fluorinated layer on conventional hydriding alloy surfaces. The aim of this paper is to elucidate the fluorination effects of La-incorporated Ti/Zr-based AB_2 laves phase alloys on the surface properties regarding their activation characteristics in gas–solid and electrochemical reactions through ESCA, EPMA, XRD studies and microscope observation. The results are to be correlated with former studies on the fluorinated AB_5 alloys, i.e. $LaNi_{4.7}Al_{0.3}$. The roles of Ni on the surface of both the AB_2 phase and La-enriched second phase before and after the fluorination will be described in this paper.

Keywords: Fluorination procedure; Surface catalysis; AB_2 laves phase; La-enriched secondary phase; Hydrides

1. Introduction

Many efforts have been made in recent years [1–4] to improve the poor activation characteristics of multicomponent Ti/Zr-based AB_2 compounds, which have been extensively developed not only as hydrogen storage materials but also as electrode materials for Ni–MH batteries, because of their better H-capacity and corrosion resistance comparing with those of rare earth-based AB_5 alloys [5,6].

The Ti/Zr-based AB_2 powder surface is easily oxidized by forming very dense Zr- and/or Ti-oxides which impede the catalytic dissociation of $H_2 \rightarrow 2H$ in gas–solid reactions or $H^+ \rightarrow H$ in electrochemical reactions.

One of the important roles of the fluorination procedure is to remove the oxide layer from the surface at the initial part of treatment, and to form a fluoride layer which improves activation characteristics drastically [7,8].

As the AB_2 alloys do not form a stable fluoride layer like LaF_3 on $LaNi_{4.7}Al_{0.3}$ surface, it is the primary aim of this study to design the fluorinated surface structure on Ti/Zr-based AB_2 alloys regarding its roles during hydrogen uptake. As one of the approaches for forming an insoluble fluorinated surface on the AB_2 compounds, small amounts of La are incorporated stoichiometrically and non-stoichiometrically, and the effects were demonstrated with great improvement in the initial activation characteristics in both the gas–solid and liquid–solid reactions.

2. Experimental procedures

2.1. Alloy preparation

The AB_2 alloys chosen in this study are based on the $(Ti,Zr)(Mn,Cr,Ni)_2$ system for gas–solid reactions and $(Ti,Zr)(V,Mn,Cr,Ni)_2$ system for electrochemical reactions. We partially substituted La equally to Ti and Zr stoichiometrically in the $Ti_{0.5-x/2}Zr_{0.5-x/2}La_xMn_{0.8}Cr_{0.8}Ni_{0.4}$ alloy and non-stoichiometrically in the $Zr_{1.0}Ti_{0.2}La_xV_{0.1}Mn_{0.7}Cr_{0.1}Ni_{0.7}$ alloy by varying the La-content x from 0 to 0.1.

Alloy samples were prepared from the elements by arc melting. Each 25 g specimen was melted 4 times to insure homogeneity, but no further annealing treatment was performed.

Metallographic studies on these La-incorporated AB_2 alloys showed that La cannot substitute into the AB_2 laves phase, but form a La-enriched secondary phase homoge-

*Corresponding author.

0925-8388/97/$17.00
PII S0925-8388(96)03031-9

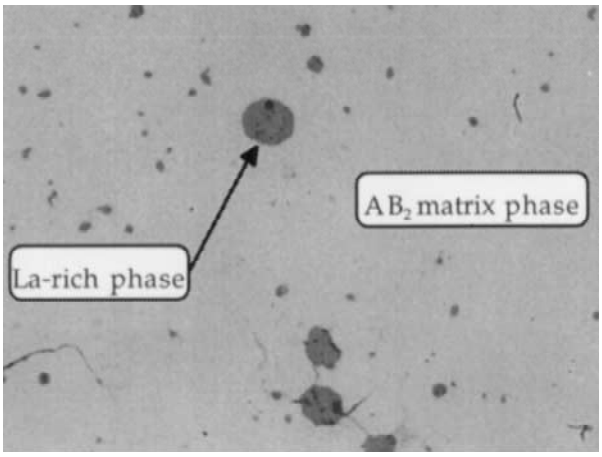

Fig. 1. Metallographic microstructure of the La-incorporated $Ti_{0.475}Zr_{0.475}La_{0.05}Mn_{0.8}Cr_{0.8}Ni_{0.4}$ alloy (orignal maginification ×1000).

neously distributed in the AB_2 matrix, as illustrated in Fig. 1.

2.2. Fluorination procedure

The F-solution is an over-saturated aqueous solution prepared by dissolving potassium fluoroaluminate (K_3AlF_6) powder into deionized water. It is a weak acidic F^--containing aqueous solution that reacts easily with the alloy surface forming the fluorinated layer [9].

During fluorination, a series of chemical reactions between the F^--ions and the alloy surface is involved resulting in the formation of a fluoride layer after reduction of the oxides, as illustrated in the following equations taking $(Ti,Zr)(Mn,Cr,Ni)_2$ as an example. La fluoride (LaF_3) is the only fluoride found during the reaction. On the other hand, other components in AB_2 alloys only form soluble fluorides which are dissolved into the F-solution as stable complex anions.

$$ZrO_2 + TiO_2 + 12F^- + 8H^+ = [TiF_6]^{2-} + [ZrF_6]^{2-} + 4H_2O \quad (1)$$

$$La_2O_3 + 6F^- + 6H^+ = 2LaF_3(\text{insoluble}) + 3H_2O \quad (2)$$

$$Ni + Mn + 10F^- + 2H_2O = [NiF_6]^{4-} + [MnF_4]^{2-} + H_2\uparrow/2H(\rightarrow MH_x) + 2OH^- \quad (3)$$

$$2Cr + 3F^- + 2H_2O = CrF_3(\text{slightly soluble}) + Cr^{++} + H_2\uparrow/2H(\rightarrow MH_x) + 2OH^- \quad (4)$$

These reactions will decrease the concentration of H^+ ions in the F-solution and form a hydride on the alloy surface (MH_x) or to form H_2 gas ($H_2\uparrow$), as a result of the pH increase.

3. Results and discussions

3.1. Electrochemical activity in liquid–solid reaction

In order to avoid Ni dissolution into the F-solution during the fluorination treatment (see Eq. (3)), Ni^{2+} was added into the F-solution which is reduced to metallic Ni on the surface of the La-incorporated and fluorinated $(Ti,Zr)(V,Mn,Cr,Ni)_2$ alloy [10]. This alloy shows an excellent initial discharge capacity, compared to that of the original alloy (see Fig. 2(A)). The inital discharge capacity was further improved under an increased discharge current density as shown in Fig. 2(B).

The results are due to the higher electrochemical activity at the fluorinated surface of the La-enriched secondary phase where it is associated with metallic Ni to form a $LaNi_x$ phase, as reported in the previous studies [11], and the metallic Ni-enriched surface of the AB_2 phase.

La-incorporated AB_2 alloys form the porous and H-transport oxide on the La-enriched $LaNi_x$ secondary phase.

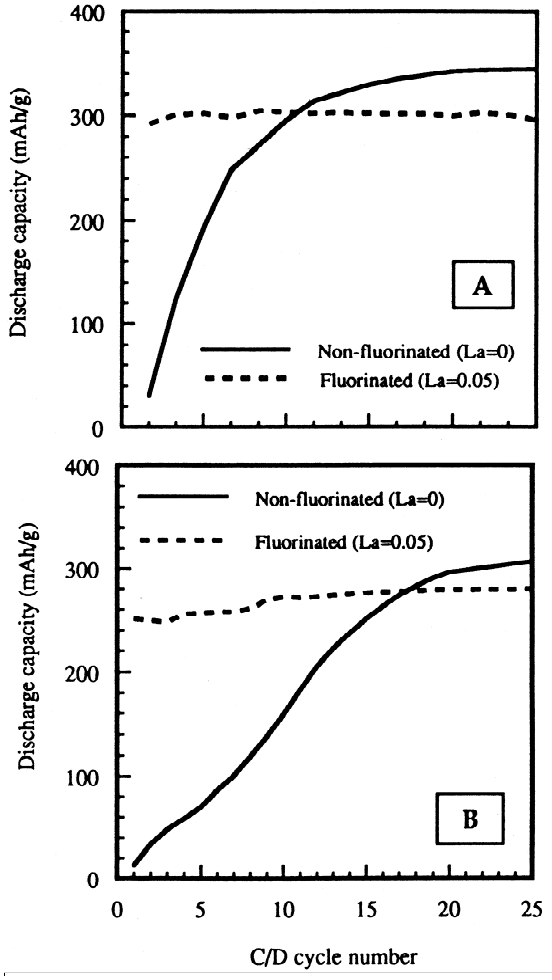

Fig. 2. La-incorporation effect of the $Zr_{1.0}Ti_{0.2}La_xV_{0.1}Mn_{0.7}Cr_{0.1}Ni_{0.7}$ ($x = 0, 0.05$) alloy on the inital activation at 20 °C. (A) discharge at 50 mA g^{-1}, (B) discharge at 150 mA g^{-1} (charge 200 mA g^{-1} for 3 h, rest 10 min, discharge to −0.6 V vs. Hg/HgO).

The metallic Ni is segregated in the near surface as has been observed in AB_5-type alloys [12]. The grain boundaries between $LaNi_x$ and AB_2 phases provide paths for hydrogen to penetrate into the interior so as to improve the initial electrochemical activation. Additionally, it has been found that the discharge capacity is reduced by the formation of a second phase, i.e. $LaNi_x$ phase.

3.2. Activation behavior in gas–solid reaction

La-incorporation to AB_2 alloys improves significantly the H_2 activation characteristics, as shown in Fig. 3. Increasing La-contents result in an increase of the reaction kinetics, although the $x=0.0$ sample cannot be activated at all, even after 24 h at 1.0 MPa H_2 pressure. However, no further obvious improvement can be observed after a level of La-content higher than 0.05.

The La-enriched secondary phases homogeneously distributed in the AB_2 phase serve as the ''gate'' for hydrogen uptake both at the surface of alloy particles and the interfaces between the grain boundaries.

On the other hand, the fluorination treatment enhances the activation kinetics compared with the untreated samples as shown in Fig. 3. Fluorination gives duplicated effects on the reaction kinetics in addition to the incorporation of La to the AB_2 compounds. This effect has to be attributed to the formation of the La-fluoride layer which is known to exhibit a high affinity to hydrogen, as proved in the $LaNi_{4.7}Al_{0.3}$ alloy [7,8].

3.3. Surface property

In order to clarify the fluorination effects and the roles of metallic Ni in the surface region on the surface properties of the La-incorporated AB_2 alloys, the surface compositions and the chemical states of constituent elements at the surface of both the AB_2 and La–Ni phases in La-incorporated $Ti_{0.5-x/2}Zr_{0.5-x/2}La_xMn_{0.8}Cr_{0.8}Ni_{0.4}$ ($x=$ 0, 0.05) alloys before and after fluorination have been studied by means of XPS and EPMA at different sample depths.

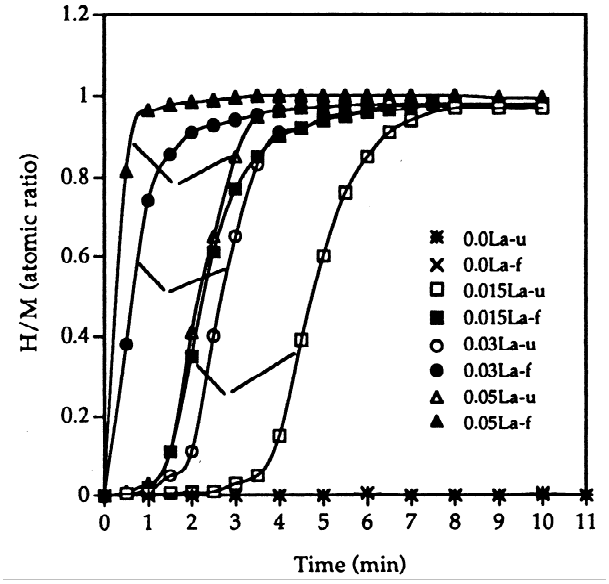

Fig. 3. La-incorporation effect of the $Ti_{0.5-x/2}Zr_{0.5-x/2}La_xMn_{0.8}Cr_{0.8}Ni_{0.4}$ ($x=0$–0.05) alloy on the initial H_2 activation (temp. −40 °C, pressure 1.0 MPa after 30 min vacuum).

3.3.1. Surface composition and chemical state of the AB_2 phase ($La=0$)

The XPS analysis has been carried out with a Mg Kα ($h\nu-1253.6$ eV) radiation and a base pressure of 10^{-7} Pa. The results are shown in Fig. 4. It can be seen that both the samples before and after the fluorination are strongly oxidized to ZrO_2 and TiO_2 at the surface. Before fluorination (see the upper part in Fig. 4), Zr is oxidized to a considerable depth, but TiO_2 persists only on the top-layers. It changes into the metallic state with increasing sample depth. Little Mn-oxide was detected besides metallic Mn. Ni and Cr which exist in a metallic state dominate the sub-layers.

After fluorination (see the lower part in Fig. 4), ZrO_2 and TiO_2 are observed even after prolonged sputtering, i.e. at greater depth. The spectrum of the Ni 2p core level indicates that NiO and metallic Ni coexist in the top-layers, but the portion of metallic Ni increases with increasing depth. Cr was detected as metallic Cr with only very limited Cr-fluoride, identified as CrF_3. Mn was difficult to observe at the top-layer. However, only small F signals are found in the surface, and no fluoride compound was clearly found in the non-La-incorporated AB_2 alloys. In contrast, the AB_2 phase seems to form more passive oxides, obviously due to air-exposure during the drying process.

Using the cross section of the Ti 2p, Zr 3d, Mn $2p_{3/2}$, Cr 2p and Ni $2p_{3/2}$ core levels after 2 min sputtering, the atomic ratios of Ti^0 to Zr^0, Mn^0, Cr^0 and Ni^0 were quantitatively determined. The calculated data show that the top-surface composition of the original $Ti_{0.5}Zr_{0.5}Mn_{0.8}Cr_{0.8}Ni_{0.4}$ alloy was changed from the untreated $Ti_{0.5}Zr_{0.65}Mn_{0.42}Cr_{2.07}$ $Ni_{0.89}$ into the treated $Ti_{0.5}Zr_{0.27}Mn_{0.36}Cr_{1.28}Ni_{0.90}$ by indicating a change of the surface composition from (Zr,Cr)-rich into Ni-rich after the fluorination treatment.

3.3.2. Surface composition and chemical state of the La-rich secondary phase ($La=0.05$)

XPS spectra of the fluorinated La-incorporated $(Ti,Zr)(Mn,Cr,Ni)_2$ alloy ($x=0.05$) indicated a La-fluoride (LaF_3) formed on the surface in addition to the formation of a Ni-enriched AB_2 matrix surface (see the lower part of Fig. 4). The result is consistent with the spectra of La $3d_{5/2}$ core level for LaF_3 and the spectra of F 1s core level studied in $LaNi_{4.7}Al_{0.3}$ [13].

3.3.3. Element X-ray images by EPMA

The EPMA analysis confirmed the above stated result in ''b'', as can be seen in Fig. 5, which shows isolated

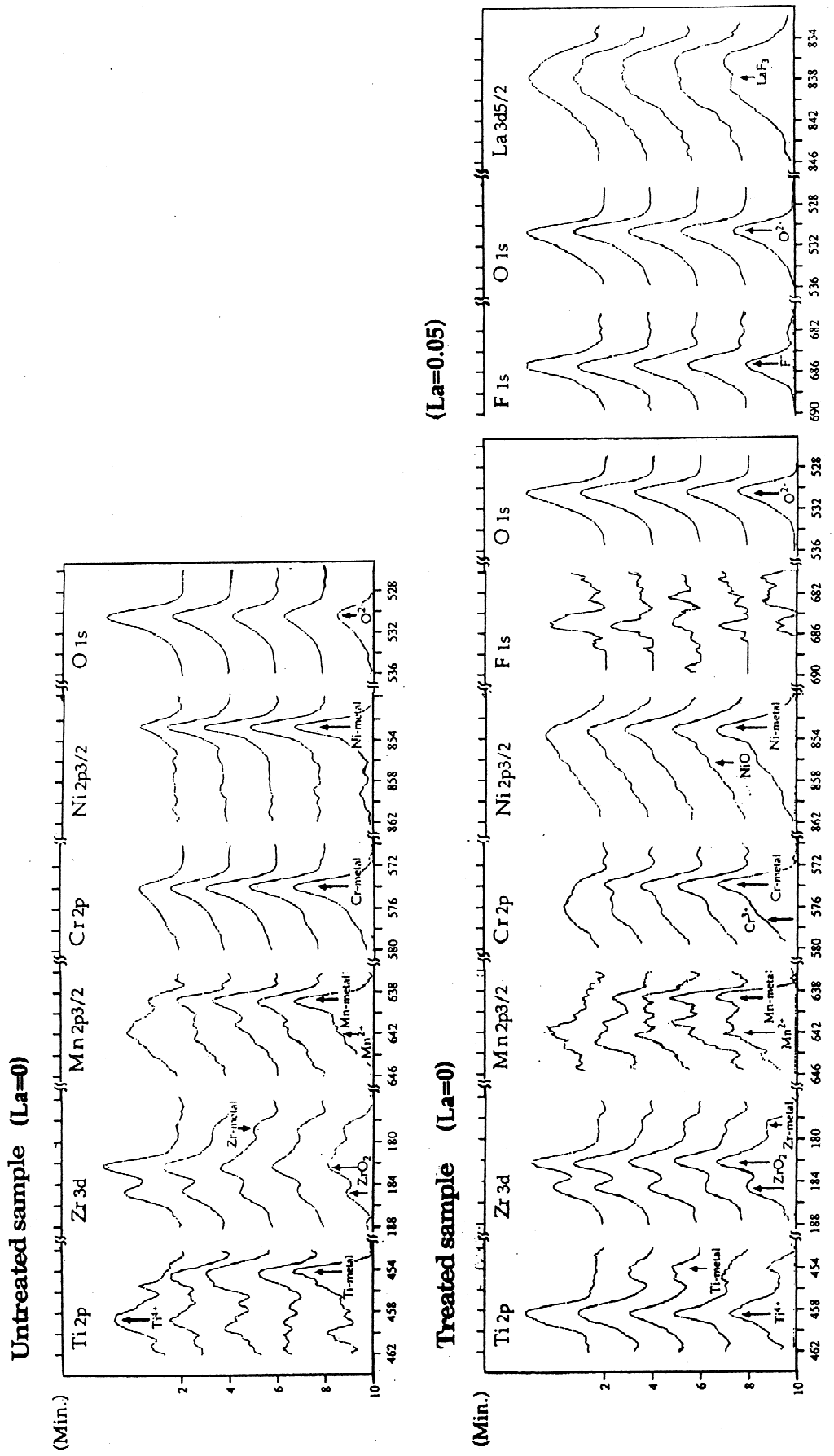

Fig. 4. XPS spectra for Ti 2p, Zr 3d, Mn 2p, Cr 2p, Ni 2p, O 1s, La 3d and F 1s core level of $Ti_{0.5-x/2}Zr_{0.5-x/2}La_xMn_{0.8}Cr_{0.8}Ni_{0.4}$ ($x=0$, 0.05) alloys at different sputting times (upper part-before fluorination, lower part-after fluorination).

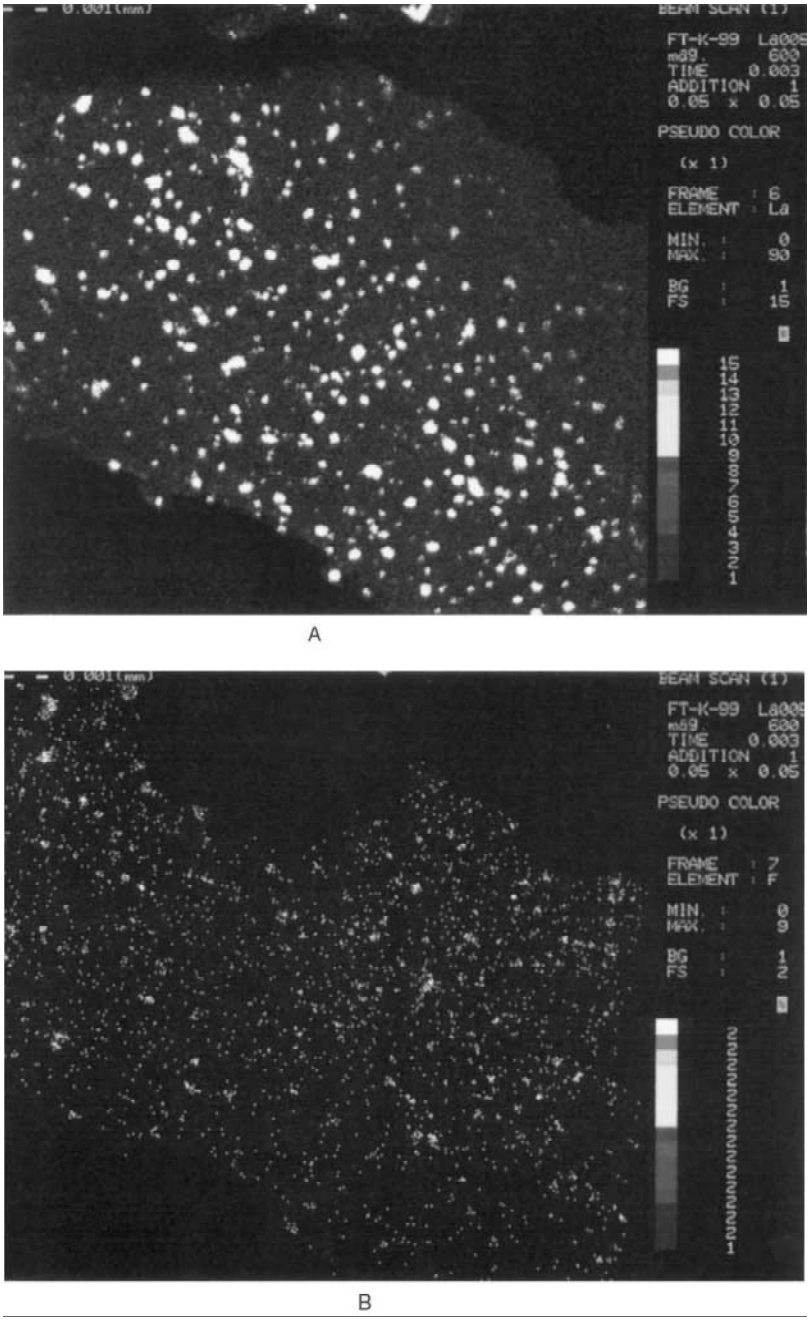

Fig. 5. Surface elemental X-ray images of the fluorinated $Ti_{0.475}Zr_{0.475}La_{0.05}Mn_{0.8}Cr_{0.8}Ni_{0.4}$ alloy particle (La and F).

La-rich phases dispersed on the particle surface and forming the La-fluoride after the fluorination. It is understood that the La-incorporation does not result in a whole coverage of the AB_2-matrix with a protective LaF_3 layer during fluorination, as have been observed in the $LaNi_{4.7}Al_{0.3}$ alloy. Formation of La-fluoride is restricted only at the parts of the La-containing secondary phases. In contrast, the AB_2 phase that is usually covered by Zr- and/or Ti-oxides did not form a metallic fluoride layer on the surface, such as LaF_3 in the case of $LaNi_{4.7}Al_{0.3}$.

3.4. Improved activation mechanism

The fluorination procedure enriches the Ni-content in the surface composition of the AB_2 phase, which is known to improve the hydriding characteristics at least in the metallic state. This is brought by the selective dissolution of the elements from the particle surface into F-solution as described in Eqs. (1)–(4) and the detailed information collected by ICPS analysis by tracing the concentration change of metallic ions in the F-solution during the

treatment. Zr was found to dissolve easily into the F-solution with the order of Zr>Ti>Mn>V>Ni>Cr. Among all the constituents, Cr was found to be the slowest component to dissolve in the F-solution.

As the elements are being dissolved from alloy particles, a large amount of cavities with holes at the surface are found (see the SEM picture in Fig. 6). Such a surface structure is known to increase the specific surface area, thus, to accelerate the reaction kinetics.

Metallic Ni on the alloy surface exists as NiO due to the air-exposure during drying after fluorination, and NiO is changed in turn to $Ni(OH)_2$ in the KOH electrolyte and easily reduced to metallic Ni during charging, which may cause the improvement of the electrochemical activity. However, in the gas–solid reaction, NiO is difficult to reduce to metallic Ni, especially under the moderate temperature and pressure conditions applied in this experiment.

Therefore, the fluorination procedure cannot demonstrate the same improvement of activation in the gas–solid reaction as it did in the liquid–solid reaction without formation of the fluorinated surface in the non-La-incorporated AB_2 compounds, which protect the sample against air-exposure.

La-incorporation results in the formation of a La-enriched secondary phase, distributed in the AB_2 phase which provides reactive sites for dissociation of H_2 molecules into atoms in the gas–solid reaction or the reduction of ionic hydrogen to atoms in the electrochemical reaction. A significant effect can be further expected by forming the La-fluoride layer in addition to the Ni-enrichment effect.

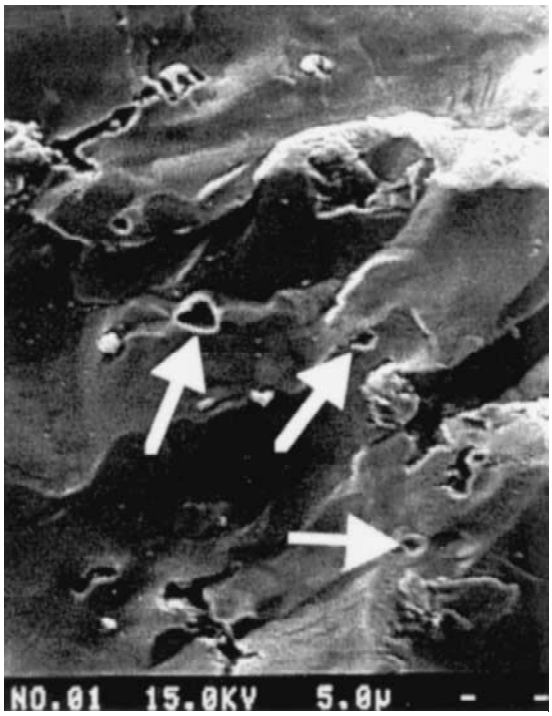

Fig. 6. SEM picture showing the surface morephology of the fluorinated $Ti_{0.475}Zr_{0.475}La_{0.05}Mn_{0.8}Cr_{0.8}Ni_{0.4}$ alloy.

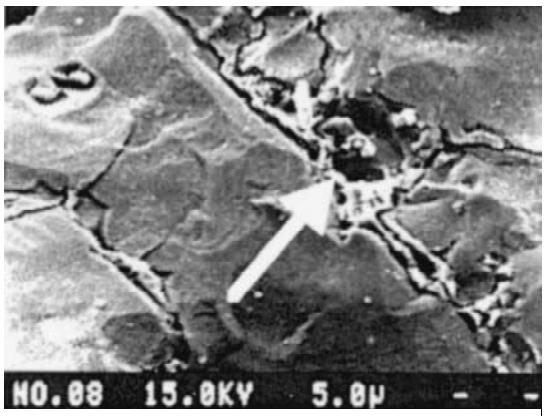

Fig. 7. SEM picture of a cross-section of the fluorinated $Ti_{0.475}Zr_{0.475}La_{0.05}Mn_{0.8}Cr_{0.8}Ni_{0.4}$ alloy after initial H_2 activation at 40 °C.

During initial activation, the grain boundaries between the La-rich phase and the AB_2 matrix play an important role for allowing H-permeation into the AB_2 lattice. Simultaneously, La-rich phases also act as the crack generating sites for creating new micropasses. These micropasses may increase the specific surface area of powders and accelerate the pulverization to stabilize H/D reactions in an early stage. This effect can be seen in Fig. 7.

It becomes clear that the fluorination procedure is significantly effective for the increase of Ni distribution at the surface of the AB_2 phase and the formation of fluoride in the La-enriched secondary phase, individually.

4. Conclusion

1. A small amount of La-incorporation makes it possible to produce fluorinated AB_2 hydriding alloys with a high reactivity and permeability of hydrogen which exhibit significant improvement of the initial activation both in the gas–solid and the liquid–solid reactions.
2. The fluorination procedure is effective for the increase of Ni distribution at the surface of the AB_2 phase and the formation of a fluoride layer on the La-enriched secondary phase, individually.
3. La-incorporation effects can be replaced by the Ce or Mm (mischmetal) incorporation.
4. The fluorination procedure should be applied in future developments to other hydriding alloys which have poor activation characteristics, such as TiFe and Mg-based alloys, in order to improve the hydrogen uptake process.

References

[1] S. Wakao, H. Sawa, H. Nakano, S. Chubachi and M. Abe, *J. Less-Common Met.*, *131* (1987) 311
[2] S. Wakao and H. Sawa, *J. Less-Common Met.*, *172–174* (1991) 1219, and *Materials Transactions: JIM, 31* (1990) 487.
[3] M.A. Fetcenko, S. Venkatesan and S.R. Oveshinsky, *Electrochem. Soc. Proc.*, *92* (1992) 141.
[4] X.-P. Gao, D.-Y, Song, Y.-S. Zhang, Z.-X. Zhou, W. Zhang, P.-W. Shen and M. Wang, *J. Alloys Comp.*, *231* (1995) 582.
[5] B.K. Zitos, D.L. Hudson, P.D. Bennett and V.J. Puglisi, *Electrochem. Soc. Proc., 92* (1992) 168.
[6] T. Sakai, H. Miyamura, N. Kuriyama, A. Kato, K. Oguro and H. Ishikawa, *J. Electrochem. Soc.*, *137* (1990) 795.
[7] F.-J. Liu, G. Sandrock and S. Suda, *J. Alloys Comp.*, *190* (1992) 57.
[8] F.-J. Liu and S. Suda, *J. Alloys Comp.*, *232* (1995) 212.
[9] F.-J. Liu, A study on the properties and characteristics of fluorinated hydriding alloys in gas–solid reaction, *Ph.D. Thesis*, 1996, Chapter 3.
[10] S. Suda, Jpn. Patent, No. 4-199231, 1992 and No. 8-118098, 1996.
[11] F.-J. Liu, G. Sandrock and S. Suda, *J. Alloys Comp.*, *231* (1995) 392.
[12] L. Schlapbach, A. Seiler, H.C. Siegmann, T.V. Waldkirch and P. Zurcher, *Int. J. Hydrogen Energy*, *4* (1979) 21.
[13] X.-W. Wang and S. Suda, *Z. Phys. Chem.*, *183* (1994) 385.